Effect of aging time and Al substitution on the morphology of aluminous goethite

Haibo Liu[a,b], Tianhu Chen[a,*], Ray L. Frost[b,*], Dongyin Chang[a], Chengsong Qing[a], Qiaoqin Xie[a]

[a] School of Resource and Environmental Engineering, Hefei University of Technology, China;

[b] School of Chemistry, Physics and Mechanical Engineering, Science and Engineering Faculty, Queensland University of Technology, Australia.

Abstract:

Goethite and Al-substituted goethite were synthesized from the reaction between ferric nitrate and/ or aluminum nitrate and potassium hydroxide. XRF, XRD, TEM with EDS were used to characterize the chemical composition, phase and lattice parameters, and morphology of the synthesised products. The results show that d(020) decreases from 4.953 Å to 4.949 Å and the *b* dimension decreases from 9.951 Å to 9.906 Å when the aging time increases from 6 days to 42 days for 9.09 mol % Al-substituted goethite. A sample with 9.09 mol% Al substitution in Al-substituted goethite was prepared by a rapid co-precipitation method. In the sample, 13.45 mol%, 12.31mol% and 5.85 mol% Al substitution with a crystal size of 163, 131, and 45 nm are observed as shown in the TEM images and EDS. The crystal size of goethite is positively related to the degree of Al substitution according to the TEM images and EDS results.

* Author to whom correspondence should be addressed Tianhu Chen (chentianhu1964@126.com; chentianhu168@vip.sina.com); and
Ray L. Frost (r.frost@qut.edu.au); P +61 7 3138 2407 F: +61 7 3138 1804

Thus, this methodology proved to be effective to distinguish the morphology of goethite and Al substituted goethite.

Keywords:

Goethite, Al substitution, Morphology, Aging time, Unit cell dimension

1. Introduction

Goethite (α-FeOOH) occurs in rocks and throughout the various parts of the global ecosystem and is frequently used as an important raw material to produce magnetic iron oxide and pigments [1-3]. The structure of goethite is similar to that of gibbsite containing essentially layers of oxygen ions in the sequence of hexagonal close-packing with the iron ions in the octahedral interstices [4-7]. Goethite is the best studied example of an isomorphously substituted iron oxide (hydroxide) and of the various possible substitutions in both natural and synthetic goethite samples. The substitution of aluminum for iron in goethite was well demonstrated and has been shown to occur in natural goethites [8-15]. Al substitution amount for Fe differs from different natural goethites ranging from zero to 33 mol% [16-18]. In addition, Al-substituted goethite can also be synthesized easily in the laboratory. Thiel *et al.* [19] synthesized goethite containing about 33 mol% Al, a level recognized as the probable upper limit of Al tolerated by the goethite structure [20]. However, as much as 47 mol% Al has been reported for Al-substituted goethite synthesized from sulfate solutions [21].

It is well-known that radius of Al^{3+} (0.53Å) is slightly smaller than that of Fe^{3+} (0.65 Å) [22]. Therefore, the substitution of Al for Fe in the structure of goethite will result in the decrease of average size of the unit cell, which is related to the amount of Al substitution and is indicated by shifts of the Al-substituted goethite XRD lines to smaller d spacings. Besides, the effect of Al substitution for Fe on crystallographic structure and physicochemical properties of goethite has been researched extensively. The report of Schulze [4] indicated that the *c* dimension is a linear

function of Al substitution in the range 0-33 mol% Al, but the *a* dimension is variable over the same composition range. A linear relationship exists between the extent of Al substitution and the *a, b* and *c* edge lengths of the unit cell of synthetic goethite obtained from different ways researched by Thiel *et al.* [19], Jonas and Solymar [23], and Taylor and Schwertmann [24]. The goethite crystals become smaller as Al substitution increases and change from large polydomainic crystals to smaller, monodomainic ones [16]. On the other hand, Al substitution affects the thermal stability of goethite. Ruan *et al.* [25] reported that Al-substituted goethite in thermally more stable than non-substituted goethite based on the results of XRD and DTG and wavenumber of hydroxyl bending and stretching vibrations shifted to higher positions using FTIR technologies. As the increase of Al substitution, the dehydration temperature, the OH stretching wavenumber and the position of both OH bending vibrations increase. Besides, many researches on the effect of Al substitution on unit cell dimension, hydroxyl units, and dehydration temperature of goethite have been reported [17, 26].

However, no report on the effect of Al substitution on the morphology of goethite using TEM, especially, for one sample prepared in the same way. As is well-known, the morphology of clay minerals plays a crucial role in adsorption of environmental pollutions such as phosphorus, lead, etc. Thus, the objectives of the paper are to make it clear that the effect of aging time on unit cell dimension of Al-substituted goethite and to show the changes of morphology with an increase of Al substitution in one sample prepared under the absolute same conditions. EDS was used to measure the Al substitution in the structure of goethite.

2. Experimental

2.1 Synthesis of goethite and Al-substituted goethite

Preparation of goethite

100g of $Fe(NO_3)_3 \cdot 9H_2O$ and 400mL deionized water were placed in a 1000 mL beaker. $Fe(NO_3)_3 \cdot 9H_2O$ was dissolved by stirring continuously. After dissolution, KOH with a concentration of 5 mol/L and a concentration of 0.1 mol/L were used to regulate the pH at 13.9±0.1 pH units. After finishing the above, the beaker was sealed with film to prevent evaporation and placed in a thermotank controlled at 70 ^{o}C. After 6d, the beaker was taken out to removal of excess KOH by centrifugation several times until the pH comes to 7 pH units or so. After centrifugation, the deposits were dried at 105^{o}C, cooled to room temperature and ground to obtain powder for further characterization. The sample was labeled as synthetic goethite (SG-6)

Preparation of Al-substituted goethite

9.378g of $Al(NO_3)_3 \cdot 9H_2O$ and 90.905g $Fe(NO_3)_3 \cdot 9H_2O$ were placed in a 1000 mL beaker and then 400 mL deionized water were put into the beaker. The $Al(NO_3)_3 \cdot 9H_2O$ and $Fe(NO_3)_3 \cdot 9H_2O$ were dissolved by stirring continuously. After dissolution, KOH with a concentration of 5mol/L and a concentration of 0.1mol/L were used to regulate the pH at 13.9±0.1 pH units. After adjust of pH, the mixture was divided into five beakers. These beakers were sealed with film to prevent evaporating, put into thermotank controlled at 70 ^{o}C and kept for 6, 11, 17, 23, 42 days. After the selected aging time, redundant KOH had to be removed by centrifugation for every sample. After centrifugation, the deposits were

dried at 105 ^{o}C, cooled to room temperature, and ground to obtain powder for further characterization. The samples were labeled as SAG-10-x (x=6, 11, 17, 23, 42), namely, 10 mol% Al substitution for Fe in goethite was aged for x days. In fact, the sample proved an Al substitution of 9.06 mol% (10 mol% Al substitution in theory, Al / (Al+Fe)). The Al substitution amount is calculated by the Chemical composition measured on a Shimadzu XRF-1800 with Rh radiation.

2.2 XRD

XRD patterns were recorded using Cu Kα radiation (λ = 1.5406 Å) on a Philips PANalytical XPert Pro muti purpose diffractometer. The tube voltage is 40kV and the current, 40mA. All XRD diffraction patterns were taken in the range of 10-70^{o} at a scan speed of 2◦ min^{-1} with 0.5^{o} divergence slit size. Phase identification was carried out by comparison with those included in the Inorganic Crystal Structure Database (ICSD). The following formula was used to calculate the unit cell dimensions (UCD) because goethite was orthorhombic,

$d_{hkl} = \frac{abc}{\sqrt{b^2c^2h^2 + a^2c^2k^2 + a^2b^2l^2}}$, where h, k, l represent the crystalline face parameters and a, b, c represent the unit cell parameters.

2.3 BET

13-point BET-nitrogen isotherms were used to quantify changes in the specific surface area. All samples were degassed at 110^{o}C for 12h before analysis were conducted. The multi-point BET surface area of each sample was measured at atmospheric pressure using TriStar Ⅱ 3020

Surface Area and Pore Size Analyzer. The adsorption isotherms achieved a p/p_o range of 0.009-0.25.

2.4 TEM and EDS

Transmission electron microscope (TEM) measurements were performed on JEM-2100 with an energy dispersive X-ray (EDS) facility. The sample was mixed with alcohol and deposited on a Cu grid. Images of the microstructure and the relevant selected area electron diffraction patterns are acquired using an analytical electron microscope.

3. Results and discussion

3.1 Effect of aging time on Al-substituted

Fig. 1 reports the XRD patterns of synthetic goethite, synthetic Al-substituted goethite at an elevated aging time, and goethite from the ICSD data base (96-900-2159). These reflections ((020), (110), (120), (130), (111), etc) are observed and identified as goethite compared with the ICSD (96-900-2159) pattern. As shown in Fig. 1, the intensity of reflections increases with increasing aging time, which should be assigned to the re-crystallization and growth of Al-substituted goethite with aging. High degree of crystallinity gives rise to stronger diffraction intensity for a certain sample. Therefore, the stronger the reflection intensity, the longer the aging time.

In addition, the effect of Al substitution on the d-spacings of goethite reflection face and the effect of aging time on that of Al-substituted goethite are presented in Fig. 2. The d-spacings were derived from the

XRD patterns using the software of X'Pert HighScore Plus. As is shown in Fig. 2, all d-spacings of goethite reflection face derived from ICSD (96-900-2159) are lower than that of the synthetic goethite in the experiment, which should be ascribed to the different preparation methods. What is more important, all d-spacings decrease after the addition of $Al(NO_3)_3 \cdot 9H_2O$ during the preparation of goethite, which is attributed to the smaller Al^{3+} ionic radius than that of Fe^{3+}. This is in good agreement with the report [4]. Schulze [4] has reported that diffraction peaks became broad and shifted to high diffraction angle (namely smaller d spacing) with the increase of Al substitution in the structure of goethite. Especially, d-spacing of (020) reflection decreases gradually from 4.953 Å to 4.949 Å with an increase of aging time. The relationship between d(020) and reaction time is basically consistent with the formula: $d(020)=4.95452-2.67E\text{-}4\ t+3.22E\text{-}6\ t^2$ ($R^2=0.997$), where t represents aging time in the experiment. It indicates that d(020) of Al-substituted goethite has a negative relationship to aging time. However, little fluctuations are observed for other d-spacings as a function of aging time.

The UCD calculated from d-spacings using the formula above as affected by aging time and the BET results are shown in Table 1. It is noted that unit cell parameters of Al-substituted goethite decrease from 4.638 to 4.6 Å for *a* dimension, from 9.951 to 9.906 Å for *b* dimension, and from 3.022 to 3.009 Å for *c* dimension as compared with that of synthetic goethite, which is consistent with the published reports [17, 27, 28]. These researches showed that unit cell parameters of goethite decreased as the Al substitution amount in goethite increased. In addition, *b* dimension has a little decrease from 9.906 to 9.898 Å as a function of aging time. As presented in Table 1, a increase of BET from 52.931 to

188 72.628m^2/g is observed when $Al(NO_3)_3 \cdot 9H_2O$ was added in the process of
189 the preparation of goethite. The increase in BET should be considered to
190 be related to the decrease of crystallite size in goethite with the addition
191 of $Al(NO_3)_3 \cdot 9H_2O$ [17]. However, the BET decreases up to 47.392 m^2/g
192 dramatically from 72.628 m^2/g and then is maintained stable when the
193 aging time increases from 6 to 42 days. Obviously, the decrease in BET is
194 attributed to the re-crystalline and growth of Al-substituted goethite,
195 which is good agreement with the results of XRD. As well-known,
196 goethite has been proved to be a good absorbent to adsorb many potential
197 contaminants in natural such as arsenic, antimony, copper, zinc, cadmium,
198 lead, and others. [29-33] . Specific surface area plays an important role in
199 the adsorption/desorption process of goethite [34], the larger the specific
200 surface area, the greater the adsorption at a given condition. Therefore,
201 the substitution of Al and high crystallinic degree would decrease the
202 specific surface area and the adsorption amount. It is postulated that the
203 existence of Al^{3+} will have a competitive adsorption with other cations
204 and result in desorption of cations because Al substitution for Fe in the
205 structure of goethite is much easier than other cations. Maybe, this is the
206 reason why Al-substituted goethite attracted so much attention.

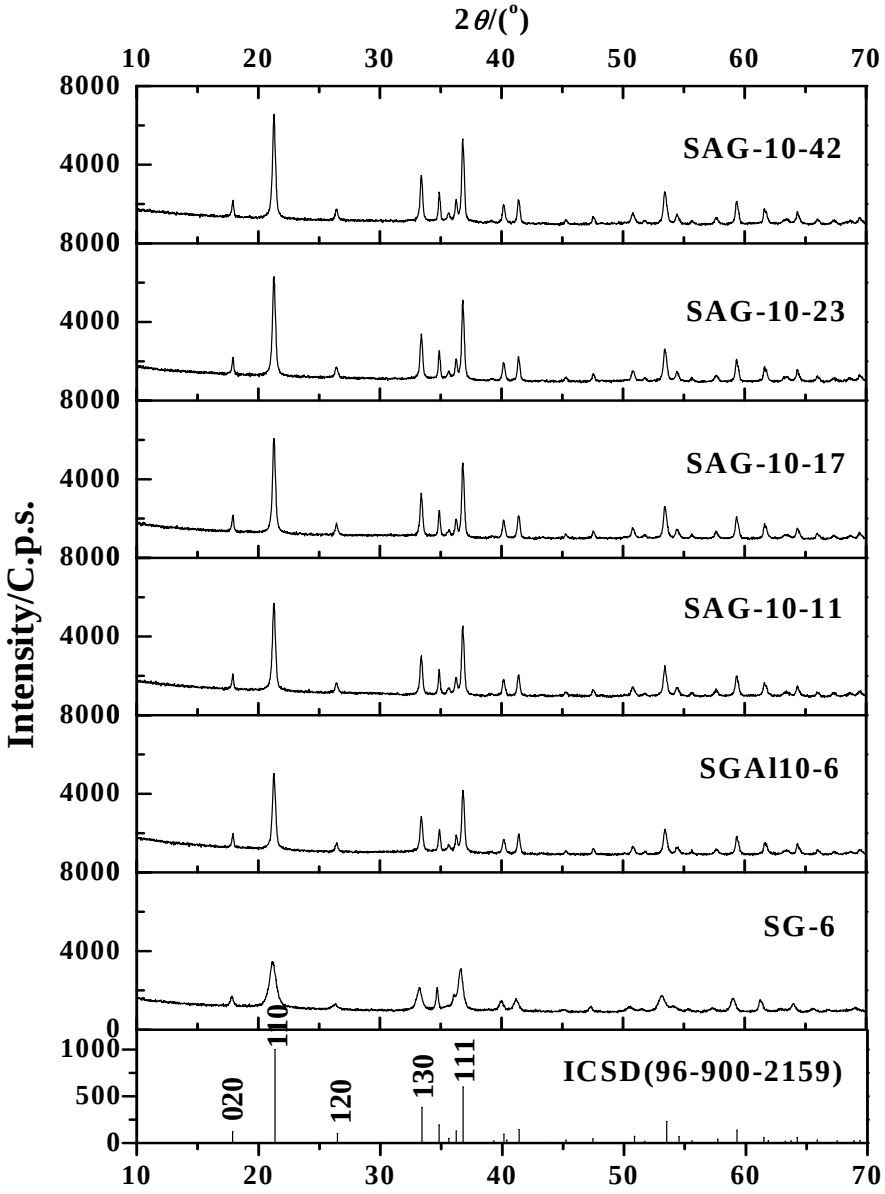

207

208 **Fig. 1. XRD patterns of goethite and Al-substituted goethite at**

209 **different** aging time

210 **Table 1. UCD and BET of goethite and Al-substituted goethite at**

211 **different aging time.**

Samples	d-spacings/Å			Unit cell parameters/Å			BET/m^2/g
	020	101	111	a	b	c	
ICSD	4.957	3.364	2.440	4.580	9.913	3.013	—
SG-6	4.976	3.378	2.454	4.638	9.951	3.022	52.9

SAG-10-6	4.953	3.365	2.440	4.600	9.906	3.009	72.6
SAG-10-11	4.952	3.368	2.439	4.594	9.904	3.007	61.9
SAG-10-17	4.951	3.371	2.441	4.611	9.901	3.007	52.5
SAG-10-23	4.950	3.370	2.441	4.607	9.899	3.009	47.4
SAG-10-42	4.949	3.368	2.443	4.597	9.898	3.014	47.2

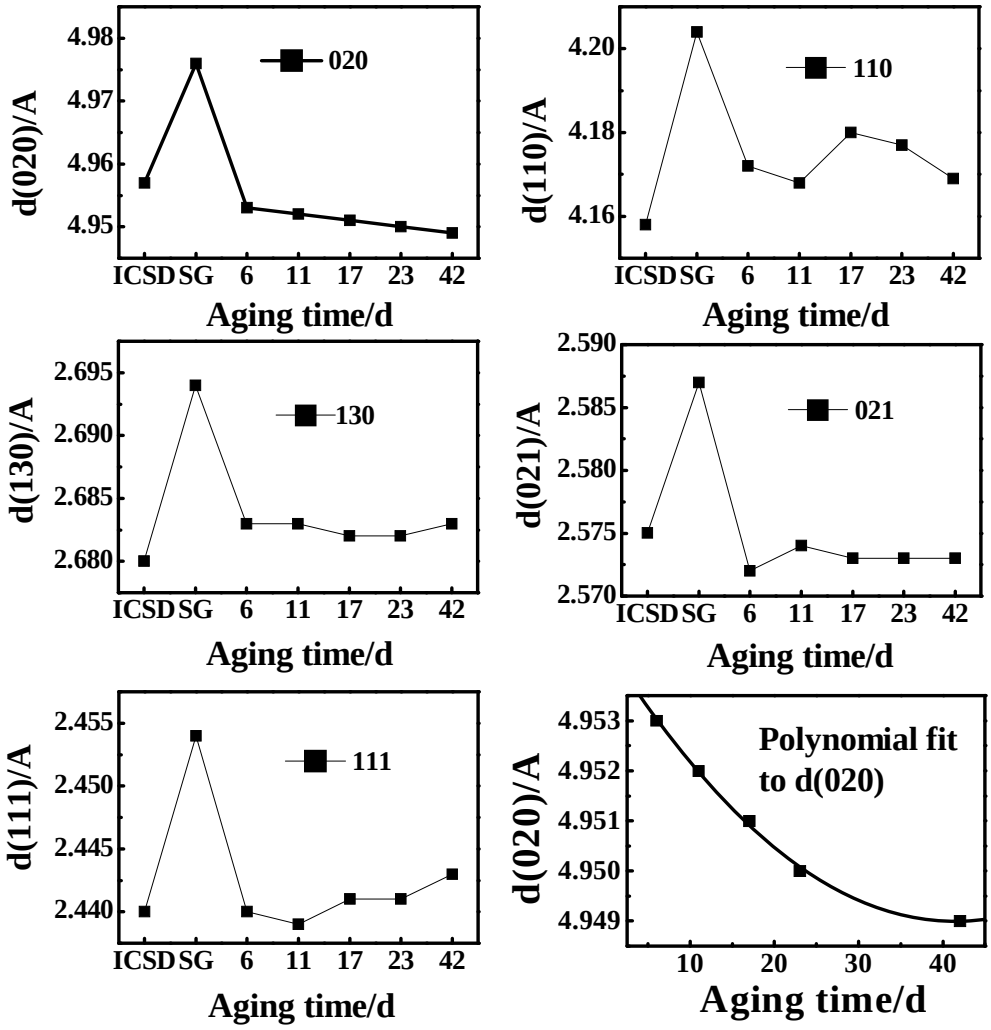

Fig. 2. d-spacings of goethite and Al-substituted goethite at different aging time.

3.2 Chemical compositions analysis

The chemical composition analysis of SG-6 and SAG-10-6 is presented in Table 2. Based on the percentage of iron and aluminum, the substitution amount of Al for Fe in goethite is calculated as 9.09 mol% compared with the theoretic value of 10 mol% which is calculated before preparation. This indicates just a little Al^{3+} was washed away due to the reaction between $Al(OH)_3$ and KOH. Meanwhile, some impurities are also detected in the synthetic Al-substituted goethite including Cr, Ca, K, etc, in which K should come from precipitator (KOH). In a word, the synthetic Al-substituted goethite main containsFe_2O_3 79.25 %, Al_2O_3 5.05 %. In contrast, almost only Fe_2O_3 84.37 % is detected in SG-6. Combined with the results of XRD, (Fe, Al)OOH is the main chemical composition for SAG-10-6 and FeOOH is the main chemical composition for SG-6 and the purity of the two kinds of goethite is over 99 wt%.

Table 2. Chemical compositions of goethite and Al-substituted goethite

Samples	Fe_2O_3	Al_2O_3	SiO_2	CaO	K_2O	Na_2O	Cr_2O_3	Loss of ignition
	%							
SG-6	84.37	0.08	0.05	0.01	—	—	0.02	14.4
SAG-10-6	79.25	5.05	0.12	0.01	2.28	0.02	0.03	13.7

3.3 Morphology of goethite with different Al substitution level

The TEM images and corresponding EDS of 10 mol% Al substitution amount for Fe in the structure of goethite is presented in Fig. 3. Some rod-like and acicular substance can be observed obviously in Fig. 3(a). These substances are confirmed to be goethite combined with the results of XRD and XRF. In addition, the results of EDS indicate these substance main contain Fe, O, Al, and Cu (deriving from copper grid). Thus, it is concluded that the synthetic products are Al-substituted goethite. However, an apparent difference in morphology can be observed in the TEM images and the materials with different morphology have different Al substitution amount for Fe based on the results of EDS with an area resolution of measurement of 500nm. According to the weight percentage of Fe and Al as determined by EDS, the Al substitution amount is calculated as 13.45 mol% for Fig. 3(c), 12.31 mol% for Fig. 3(e), and 5.85 mol% for Fig. 3(g). The corresponding crystal size is 163 nm, 131 nm, and 45nm, respectively. That is to say, the width increases with an increase of Al substitution amount. The research [17] showed dehydration temperature increased due to an increasing Al substitution, which was

ascribed to the Al^{3+} ion, retains coordinated OH more strongly than Fe^{3+} because of the higher ionic potential of Al^{3+}. The high ionic potential would attract more other ions. Therefore, goethite with more Al substitution amount has more broad width in the same aging time. Besides, the length of three selected crystal of Al-substituted goethite is observed from Fig. 3. The aspect ratio between length and width linearly decreases from 9.89 to 2.76 when Al substitution amount has an increase from 5.85 mol% to 13.45 mol%, as shown in Fig. 4. The results are consistent with the formula y=15.403-0.943x with a highly related coefficient (R^2=0.999), where y denotes the aspect ratio, x represent Al substitution amount. This illustrates that the aspect (L/W) has a negative relationship with the Al substitution amount. Why the same sample has different Al substitution amount? The reason should be ascribed to the rapid titration of KOH into the mixture of $Al(OH)_3 \cdot 9H_2O$ and $Fe(OH)_3 \cdot 9H_2O$. Obviously, it is difficult to distribute well for KOH under the condition of rapid titration. Actually, in the experiment, KOH is almost poured into the mixture and then low concentration of KOH is used to regulate the pH. The research [35] reported that the level of Al incorporation into the goethite structure is dependent on the concentration of both KOH and Al^{3+} and Al substitution amount increases with a decrease of KOH concentration at a given Al^{3+} concentration. Therefore, this rapid co-precipitation made an Al-substituted goethite with

277 considerably different Al substitution amount. Fortunately, the method
278 provides a better way to investigate the morphology of goethite with
279 different Al substitution amount in one sample, which is prepared under
280 absolutely same conditions.

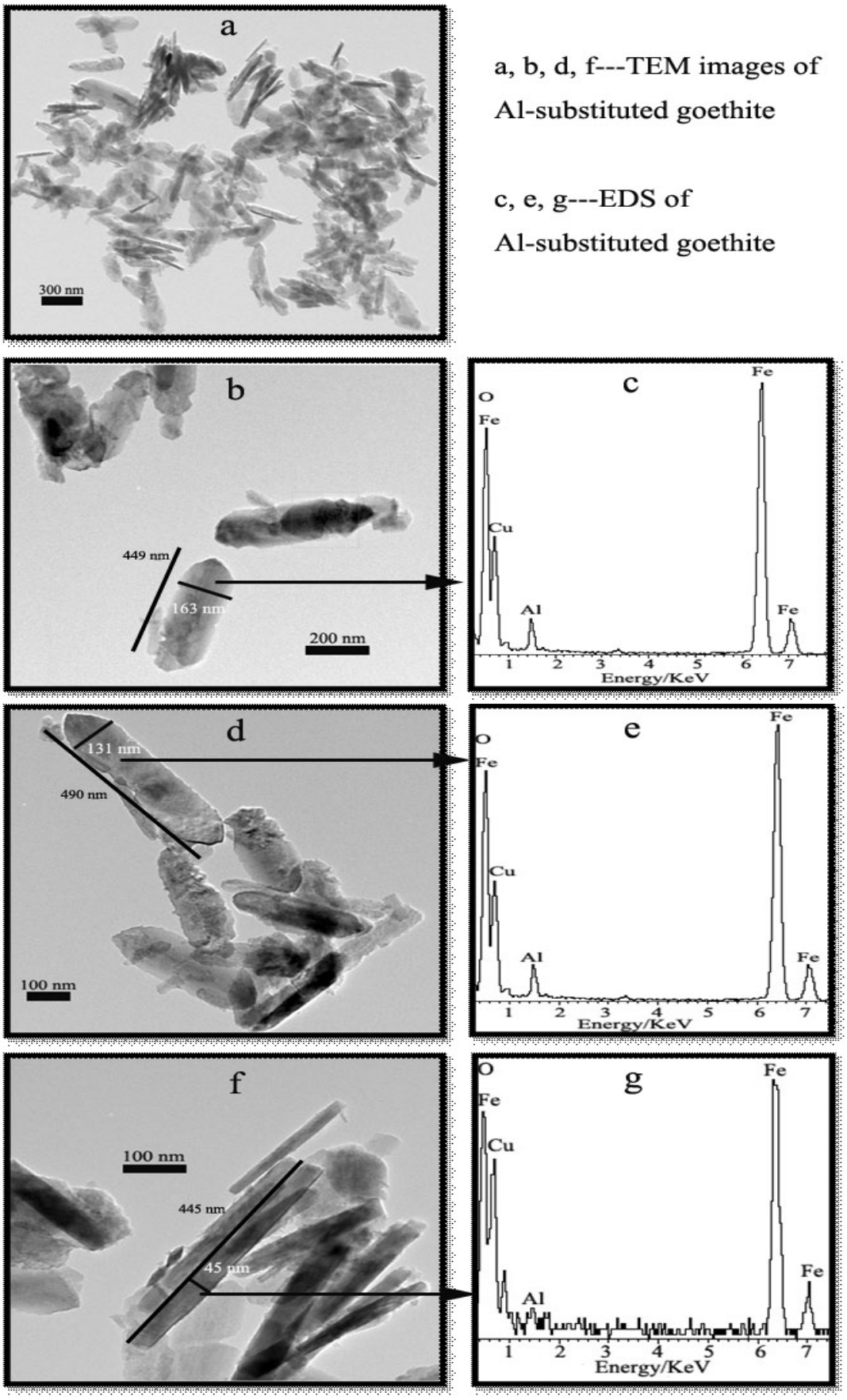
a
300 nm
a, b, d, f---TEM images of
Al-substituted goethite
c, e, g---EDS of
Al-substituted goethite
b
449 nm
163 nm
200 nm
c
O
Fe
Cu
Al
Fe
Fe
1 2 3 4 5 6 7
Energy/KeV
d
131 nm
490 nm
100 nm
e
O
Fe
Cu
Al
Fe
Fe
1 2 3 4 5 6 7
Energy/KeV
f
100 nm
445 nm
45 nm
g
O
Fe
Cu
Al
Fe
Fe
1 2 3 4 5 6 7
Energy/KeV

281

Fig. 3. TEM and EDS of SAG-10-6.

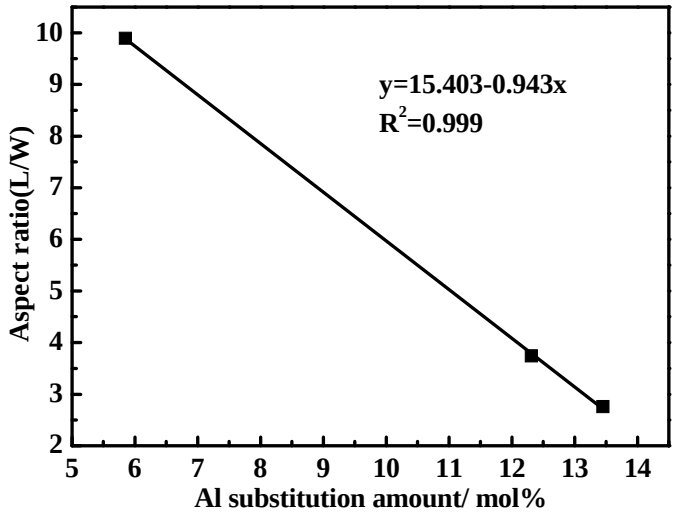

Fig. 4. Linear relationship between aspect ratio (L/W) and Al substitution amount.

4. Conclusions

Goethite and Al-substituted goethite were obtained using a rapid precipitation method. The addition of Al^{3+} decreased the unit cell parameters of goethite. d(020), *b* dimension, and specific surface area of Al-substituted goethite decreased with an increase of aging time. It was suggested the decrease of BET would make against the application of the goethite in removal of environmental pollutions. The effect of aging time of Al-substituted goethite on adsorption of environmental pollutions such as heavy metal will be investigated in the next work.

13.45 mol% Al, 12.31 mol% Al and 5.85 mol% Al-substituted goethite was gotten in one sample whose average Al substitution amount was 9.09 mol%. And the crystal width of goethite increased apparently with increasing Al substitution amount as shown in TEM and EDS. Therefore,

301 the rapid co-precipitation method provided a better way to investigate the
302 difference of crystal morphology of goethite with different Al substitution
303 amount.

304 ## 5. Acknowledgements

305 This study was financially supported by Natural Science Foundation of
306 China (No. 41172048, No. 41072035) and Ph.D. Programs Foundation of
307 Ministry of Education of China (No. 20110111110003). The authors
308 appreciate the financial and infrastructure support of the School of
309 Chemistry, Physics and Mechanical Engineering, Science and
310 Engineering Faculty, Queensland University of Technology, for this
311 research.
312

313

6. References:

[1] Qiu X., Lv L., Li G.S., Han W., Wang X.J., Li L.P. Hydrated goethite nanorods: Vibration spectral properties, thermal stability, and their potential application in removing cadmium ions. Journal of Thermal Analysis and Calorimetry, 2008, 91(3): 873-878.

[2] Jambor J. L. Occurrence and Constitution of Natural and Synthetic Ferrihydrite, a Widespread Iron Oxyhydroxide. Chemical Review, 1998, 98, 2549-2585

[3] Bikiaris D., Daniilia S., Sotiropoulou S., Katsimbiri O., Pavlidou E., Moutsatsou A.P., Chryssoulakis Y., Ochre-differentiation through micro-Raman and micro-FTIR spectroscopies: application on wall paintings at Meteora and Mount Athos, Greece. Spectrochimica Acta Part A, 1999, 56: 3-18

[4] Schulze D. G., The influence of aluminum on iron oxides VIII. Unit-cell dimensions of Al-substituted goethites and estimation of Al from them. Clays and Clay Minerals, 1984, 32(1):36-44.

[5] Ewing F.J. The crystalline structure of diaspore. Jounral of Chemical physics, 1935, 3: 203-206.

[6] Forsyth, J.B., Hedley J.G., Johnson, C.E. The magnetic structure and hyperfine field of goethite (a-FeOOH). Journal of Physics C: Solid State Physics, 1968, 1: 179-188.

[7] Szytula A. Balanda, M. Dimitrijevic, Z. Neutron diffraction studies of a-FeOOH. Physica of Status Solidi A, 1970, 3: 1033-1037

[8] Norrish, K., Taylor, R. M. The isomorphous replacement of iron by aluminium in soil goethites. Journal of Soil Science, 1961, 12:

294-306.

[9] Janot, C., Gibert, H., de Gramont, X., Biais, R. l~tude des substitutions Al-Fe dans des roches latgritiques. Bull. Soc. Fr. Mineral. Cristallogr. 1971, 94: 367-380.

[10] Davey, B. G., Russell, J. D., Wilson, M.J.. Iron oxide and clay minerals and their relation to colours of red and yellow Podzolic soils near Sydney, Australia. Geoderma, 1975: 14, 125-138.

[11] Nahon, D., Janot, C., Karpoff, A. M., Paquet, H., Tardy, Y. Mineralogy, petrography and structures ofiron crusts (ferricretes) developed on sandstones in the western part of Senegal. Geoderma, 1977: 19, 263-277.

[12] Bigham, J. M., Golden, D. C., Bowen, L. H., Buol, S. W., and Weed, S. B. Iron oxide mineralogy of well-drained Ultisols and Oxisols: I. Characterization of iron oxides in soil clays by M□ssbauer spectroscopy, X-ray diffractometry, and selected chemical techniques. Soil Science Society of American Journal, 1978, 42, 816-825.

[13] Mendelovici, E., Yariv, Sh., and Villalba, R. Aluminum-beating goethite in Venezuelan laterites. Clays and Clay Minerals, 1979, 27, 368-372.

[14] Torrent, J., Schwertmann, U., Schulze, D. G. Iron oxide mineralogy of some soils of two river terrace sequences in Spain. Geoderma, 1980 23, 191-208.

[15] Fitzpatrick, R. W., Schwertmann, U. Al-substituted goethite--an indicator of pedogenic and other weathering environments in South

364 Africa. Geoderma, 1981, 27, 335-347.
365 [16] R.M.Cornell, U.Schwertmann. The iron oxides: structure, properties,
366 reactions, occurrences and uses. Second editor, Weinheim, 2003,
367 p.42

368 [17] Ruan, H. D., Gilkes R. J., Dehydroxylation of aluminous goethite;
369 unit cell dimensions, crystal size and surface area. Clays and Clay
370 Minerals, 1995, 43(2): 196-211.

371 [18] Norrish K., Taylor R. M., The isomorphous replacement of iron by
372 aluminum in soil goethites. Journal of Soil Science, 1961, 12, 294-
373 306.

374 [19] Thiel R., Zum system a-FeOOH-a-A1OOH. Z. An-org. Allg. Chem.
375 1963, 326: 70-78.

376 [20] Schwertmann U., Taylor R. M., Iron oxides: in Minerals in Soil
377 Environments, (J. B. Dixon and S. B. Weed, editor), Soil Science
378 Society of American, Madison, Wisconsin, 1977, 145-180.

379 [21] Bronevoi, V. A., Furmakova, L. N., 1975, 104: 461-466.

380 [22] Shannon R. D., Prewitt C. T., Effective ionic radii in oxides and
381 fluorides. Acta Cryst. B, 1969, 25: 925-946.
382 [23] Jrnas K., Solymfir K. Preparation, X-ray, de-rivatographic and
383 infrared study of aluminum-substituted goethites. Acta Chim.
384 (Budapest), 1970, 66: 383-394.

385 [24] Taylor, R. M., Schwertmann, U., The influence of aluminum on iron
386 oxides. Part I. The influence of Al on Fe oxide formation from the
387 Fe(II) system. Clays and Clay Minerals,1978, 26: 373-383.

388 [25] Ruan H. D., Frost R. L., et al. Infrared spectroscopy of goethite
389 dehydroxylation. II. Effect of aluminium substitution on the
390 behaviour of hydroxyl units. Spectrochimica Acta Part A:
391 Molecular and Biomolecular Spectroscopy, 2002, 58(3): 479-491.

392 [26] Ruan H. D., Frost R. L., et al. Infrared spectroscopy of goethite
393 dehydroxylation: III. FT-IR microscopy of in situ study of the
394 thermal transformation of goethite to hematite. Spectrochimica
395 Acta Part A: Molecular and Biomolecular Spectroscopy, 2002,
396 58(5): 967-981.

397 [27] Schulze, D. G., Schwertmann U. The influence of aluminium on iron
398 oxides: XlII. Properties of goethites synthesised in 0.3 M KOH at
399 25^{o}C, Clay Minerals., 1987, 22: 83-92.

400 [28] Schwertmann U., Cambier P., Murad E. Properties of goethites of
401 varying crystallinity. Clays and Clay Minerals. 1985, 33: 369-378.

402 [29] Boily, J.F., Persson, P., Sjöberg, S., Benzenecarboxylate surface
403 complexation at the goethite (α-FeOOH)/water interface: III. The
404 influence of particle surface area and the significance of modeling
405 parameters. Journal of Colloid and Interface Science, 2000, 227 (1):
406 132-140.

407 [30] Mamindy-Pajany Y., Hurel V., Marmier N., Romeo M., Arsenic
408 adsorption ontohematite and goethite. Comptes Rendus Chimie,
409 2009, 12 (8): 876-881.

410 [31] Mitsunobu S., Takahashi Y., Terada Y., Sakata M., Antimony (V)
411 incorporation into synthetic ferrihydrite, goethite, and natural iron
412 oxyhydroxides. Environmental Science and Technology, 2010, 44
413 (10): 3712-3718.

414 [32] Swedlund P.J., Webster J.G., Miskelly G.M., Goethite adsorption of
415 Cu(II), Pb(II), Cd(II), and Zn(II) in the presence of sulfate:
416 properties of the ternary complex. Geochimica et Cosmochimica
417 Acta, 2009, 73 (6):1548-1562.

418 [33] Tribe L., Barja B. C. Adsorption of Phosphate on Goethite. An
419 Undergraduate Research Laboratory Project. Journal of Chemical
420 Education, 2004, 81(11): 1624-1627.

421 [34] Dzombak, D.A., Morel, F.M.M., Surface Complexation Modeling:
422 Hydrous Ferric Oxide. John Wiley, New York, 1990

423 [35] Lewis D. G., Schwertmann U. The influence of aluminum on the
424 formation os iron oxides. IV. The influence of [Al], [OH], and
425 temperature. Clays and Clay Minerals, 1979, 27(3): 195-200.